Tethered vesicles at constant pressure: Monte Carlo study and scaling analysis

S. Komura* and A. Baumgärtner
Institute für Festkörperforschung, Forschungszentrum Jülich, D-5170 Jülich, Federal Republic Germany
(Received 26 December 1990; revised manuscript received 16 April 1991)

Tethered vesicles at various constant pressure differences Δp are investigated by Monte Carlo simulations. Flaccid vesicles ($\Delta p=0$) exhibit uncrumpled configurations with a mean-square radius of gyration $\langle R^2\rangle_0 \sim N^{\nu}$, where $\nu \approx 1.0$ and N is proportional to the surface area. The roughness of their surfaces is characterized by an exponent $\zeta=0.65$. The crossover to inflated vesicles ($\Delta p>0$) and to deflated vesicles ($\Delta p<0$) are analyzed by means of finite-size crossover scaling assumptions. The crossover to inflated vesicles ($\nu=1.0$) is governed by the reduction of the corrugation due to the pressure, i.e., from $\zeta=0.65$ to 0, which is characterized by a crossover exponent $\varphi=1.88$. The crossover to deflated vesicles is ruled by the change of their sizes, i.e., from $\nu=1.0$ to 0.66, which is characterized by $\varphi'=4.4$.

I. INTRODUCTION

Properties of tethered networks have received great attention recently in connection with both biophysics of membranes and statistical mechanics of random surfaces [1]. Tethered membranes are realized not only in biological systems, such as the spectrin protein skeleton of eurythrocytes, but also in artificial membranes, for example, polymerized amphiphilic bilayers. In contrast to linear polymer chains, polymerized membranes may exhibit a low-temperature flat phase due to phonon-mediated long-range interactions, in spite of their two-dimensional character. This flat phase is not described by the classical theory of elasticity.

A spherically closed membrane is called a "vesicle," exemplified by red blood cells. From the experimental point of view, it is easier to prepare a single polymerized vesicle than to control the size of monodisperse ensembles of open sheets. This type of thin-walled vesicles is of current interest as models of cell membranes which exhibit many different shapes [2]. This shape transformation is caused by changing, e.g., the osmotic conditions, the composition of the lipid, or the temperature.

In the present paper, we report on Monte Carlo simulation of tethered vesicles subjected to osmotic pressure differences

$$\Delta p = p_{\text{in}} - p_{\text{out}} , \tag{1}$$

measured between inside and outside. Our simulation has been performed in ($d=3$)-dimensional space, using vesicles which have ($D \equiv d-1=2$)-dimensional tethered surfaces [3,4] (three-dimensional vesicles) as in the real world. The self-avoidance of the surface is also taken into account in our simulation, which gives rise to a certain intrinsic bending rigidity. As has been shown previously by simulation [5], this induced intrinsic bending rigidity is large enough to keep the flaccid tethered vesicles ($\Delta p=0$) uncrumpled.

On the other hand, our work may be considered as a continuation and an extension of previous studies on ($D=1$)-dimensional vesicles in ($d=2$)-dimensional space ("planar vesicles" or "ring polymers") performed first by Leibler, Singh, and Fisher [6,7] (hereafter denoted LSF). Using also the "sphere and tether model," they measured the mean-square radius of gyration and the area of the planar vesicles. Both of these quantities scale with a single correlation exponent $\nu=\frac{3}{4}$ for the flaccid case (note that they are crumpled). They showed by scaling analysis that inflated ($\Delta p>0$) vesicles become circular, while deflated ($\Delta p<0$) vesicles collapse to forms of branched-polymer structures. Planar vesicles change their shapes *continuously* and the transformations are controlled by the scaling variable $\Delta p N^{2\nu}$, where N is the number of monomers [8]. Results of a recent subsequent study for the inflated planar vesicles are well explained by Pincus's expression for the size of a stretched polymer chain [9].

We show in this paper that three-dimensional vesicles exhibit several different properties in comparison to planar vesicles. These differences originate mainly from the fact that three-dimensional "hard sphere and tether models" of vesicles are *not* crumpled in the flaccid case. It then turns out to be more important to characterize these vesicles in terms of roughness using the roughness exponent ζ. In order to make this point clear and to extend the simulations to the case of nonzero constant pressure, we repeated the simulation for $\Delta p=0$ [5]. It is also remarkable that our data cannot be described by a single crossover exponent but need different values for inflated and deflated regimes. This is due to the difference in the related crossover phenomena.

The outline of this article is as follows. First we explain our model and the simulation techniques. In Sec. III, we present the results for $\Delta p=0$, including the fluctuations of the radius of gyration and the volume. We explain their relation to the roughness of vesicle surfaces. In Sec. IV, the scaling analysis for $\Delta p>0$ is described. It will be shown that the increase of internal pressure manifests itself in the decrease of out-of-plane fluctuations. A similar scaling analysis for the crossover to the "fully collapsed" state ($\Delta p<0$) is explained in Sec. V. Comparisons of our work to previous works are made in the last section.

II. MODEL AND SIMULATION TECHNIQUES

The initial configuration of vesicles in $(d=3)$-dimensional space consists of a triangular mesh as a simplest approximation for $(D=2)$-dimensional membrane [5,10]. Starting from an icosahedron as the original network, we add new points on each triangle followed by a subsequent rescaling of all bonds to the desired length. This procedure ensures that most of the grid points have six neighbors and each bond has approximately the same length. In the present simulation we studied vesicles consisting of $N=10\times 3^k+2$ monomers with $k=1,2,3,4$ (for $\Delta p=0$, we used up to $k=5$). The number of triangles is $f=2N-4$ while the number of bonds is $e=3N-6$. These quantities surely satisfy Euler's theorem; $N+f-e=2$.

Each Monte Carlo step for vesicles consists of randomly selecting a monomer and displacing it to a nearby location, which is also chosen randomly. The energy assigned to a particular configuration of monomers with positions $\{\mathbf{r}_i\}$ in $(d=3)$-dimensional space is

$$E=-\Delta pV+\sum_{\langle i,j\rangle} v(|\mathbf{r}_i-\mathbf{r}_j|)\ . \tag{2}$$

Here V is the volume of a vesicle and the summation is over all neighboring pairs of monomers $\langle i,j\rangle$ interacting by a square-well potential, i.e.,

$$v(r)=\begin{cases}0, & a<r<l_{\max}\\ \infty & \text{otherwise}\ .\end{cases} \tag{3}$$

The parameter a represents the diameter of a hard sphere introduced on each grid point and $l_{\max}$ the maximum length of the tether ("tethered" or "polymerized membrane" [3,4]). The self-avoidance of the network and the finite extensibility of the tethers are maintained by this tethering potential. Furthermore, if $a/l_{\max}>1/\sqrt{3}$, self-interpenetration of the surface is safely prohibited [3]. In our simulation, $a=1$ and $l_{\max}=\sqrt{2}a$ are used. We fix the pressure difference Δp and let the volume V fluctuate in accordance with the Boltzmann weighting factor $\exp(-E/k_BT)$. In other words, we used the "stress ensemble" which is generally not equivalent to the "strain ensemble" [11]. Each attempted move of a monomer is set to be 0.1(a), for which about 70% of trials are accepted when $\Delta p=0$. The actual sampling of configurations is made at least every N Monte Carlo time steps (one Monte Carlo time step corresponds to N attempted moves). Since the expected correlation time between successive configurations is of the order of N^2, the collected samples are not completely uncorrelated. Equilibrium averages are taken over up to 10^4 configurations.

III. FLACCID VESICLES ($\Delta p=0$)

First we consider the case $\Delta p=0$ where vesicles exhibit flaccid conformations. This case has been studied previously for polymerized and fluid vesicles [5]. For the purpose of extending our work to the nonzero pressure regime, we have simulated this case again with more detailed analysis of the data. Some new results are incorporated in this section concerning the fluctuations of the mean-square radius of gyration and the volume in order to estimate the roughness of the surface.

A typical equilibrated sample of a polymerized vesicle at $\Delta p=0$ is depicted in Fig. 1(a). The mean-square radius of gyration $\langle R^2\rangle_0$ and the mean volume $\langle V\rangle_0$ of vesicles are expected to scale with the correlation exponents ν_R and ν_V as

$$\langle R^2\rangle_0\sim A_R^2N^{\nu_R},\quad \langle V\rangle_0\sim A_VN^{3\nu_V/2} \tag{4}$$

for large N (the subscript 0 indicates the average at $\Delta p=0$). A_R and A_V are nonuniversal amplitudes of the radius of gyration and the volume, respectively. In gen-

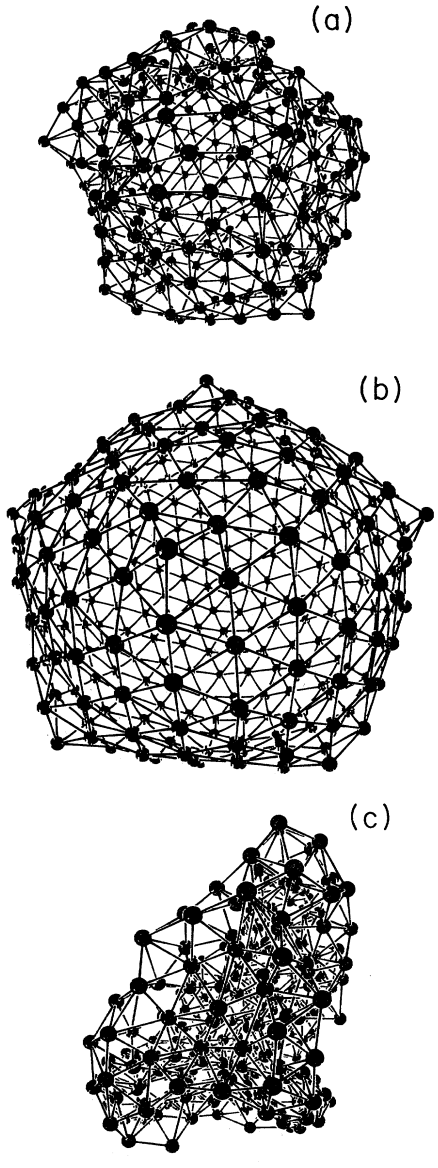

FIG. 1. Typical equilibrium configurations of polymerized vesicles for $N=272$ with (a) $\Delta p=0$ (flaccid vesicle), (b) $\bar{p}\equiv\Delta pa^3/k_BT=8.0$ (inflated vesicle), (c) $\bar{p}=-8.0$ (deflated vesicle). Size of hard spheres is reduced so that the connectivity can be easily seen.

eral, the exponent ν_R is not necessarily equal to ν_V. Note that N is proportional to the surface area.

The Monte Carlo results of $\langle R^2\rangle_0$ and $\langle V\rangle_0$ are presented in Fig. 2, from which we obtain

$$A_R^2 \simeq 0.10(a)^2, \quad A_V \simeq 0.094(a)^3 , \tag{5}$$

$$\nu_R = 0.95\pm 0.05, \quad \frac{3\nu_V}{2} = 1.48\pm 0.04 . \tag{6}$$

These results recover our previous simulation for polymerized vesicles [5] and, in particular, ν_R is in good agreement with other simulations for *open* tethered membranes [12–16] where $\nu_R \approx 1.0$. For the initial condition of the present simulation, we took not only spherical shapes described in Sec. II, but also collapsed configurations equilibrated first at $\Delta p < 0$ [compare also Sec. V and Fig. 1(c)]. Even in the latter case, vesicles will expand and the equilibrated configurations give the same exponents as shown in Eq. (6). We suspect that the difference between the values of ν_R and ν_V could be due to finite-size effects and we expect $\nu_R = \nu_V = 1.0$ in the asymptotic limit.

For planar vesicles, the relation $\nu_R = \nu_V$, where ν_V is the corresponding exponent for $(d=2)$-dimensional volume (area), was first found in the Monte Carlo simulation by LSF. This equation was later analytically derived by Duplantier using the Coulomb-gas method [17]. Our result suggests that it is also valid for three-dimensional polymerized vesicles.

The fact that the correlation exponents exhibit their upper limiting value ($\nu \le 1$) implies that polymerized vesicles without any applied pressure are essentially expanded. The shape of these expanded vesicles is estimated by the three axes of inertia $\langle \lambda_k \rangle$ $(k=1,2,3)$, which are related to the mean-square radius of gyration by

$$\langle R^2\rangle = \langle \lambda_1\rangle + \langle \lambda_2\rangle + \langle \lambda_3\rangle . \tag{7}$$

We obtained $\langle \lambda_1\rangle / \langle \lambda_3\rangle_0 \approx 0.8$ and $\langle \lambda_2\rangle_0 / \langle \lambda_3\rangle_0 \approx 0.9$, where λ_1 and λ_3 are the smallest and the largest eigenvalues, respectively. These values suggest that the shape of flaccid vesicles is close to sphericity but with weak asphericity. This view is also supported by the following ratio between the volume and the radius of gyration [7] assuming $\nu_R = \nu_V$:

$$\frac{\langle V\rangle_0}{(4\pi/3)\langle R^2\rangle_0^{3/2}} \approx \frac{A_V}{(4\pi/3)A_R^3} = 0.71 . \tag{8}$$

Note that the corresponding value for a sphere is 1.0.

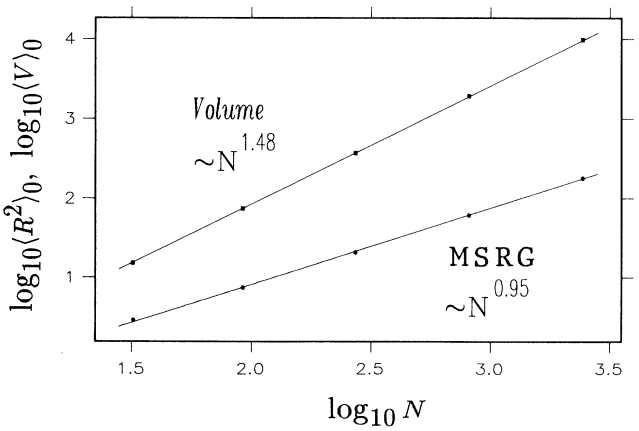

FIG. 2. Plots of the mean-square radius of gyration (MSRG) $\langle R^2\rangle_0$ and the mean volume $\langle V\rangle_0$, for the flaccid $(\Delta p = 0)$ polymerized vesicles as a function of number of monomers, N. The error bars are within the size of symbols.

Reasons why self-avoiding tethered surfaces are flat have been suggested very recently by Abraham and Nelson [18]. Due to short-range repulsive interactions between adjacent spheres of the membrane, a large bending rigidity is induced in membranes. They showed that this intrinsic bending rigidity is large enough to produce the flat phase. It is interesting to note that this behavior of three-dimensional vesicles is in contrast to planar vesicles which are *fractal* $(\nu < 1)$ with the corresponding radius of gyration $\sqrt{\langle R^2\rangle_0} \sim N^{3/4}$, where N is proportional to the contour length in this case [6–9].

Although vesicles are in the expanded shapes (with weak asphericity), their conformations are still flaccid and have not reached the fully inflated size. This implies that the surfaces of flaccid vesicles are substantially rough. The roughness of a surface is generally characterized by the out-of-plane fluctuation h whose squared average scales with the roughness exponent ζ as [19,20]

$$\langle h^2\rangle_0 \sim \frac{k_B T}{\kappa_0} L^{2\zeta} . \tag{9}$$

L is proportional to the linear length scale of the membrane size and κ_0 is the bending rigidity which, in our case, corresponds to the intrinsic bending rigidity induced by the self-avoidance effect. As mentioned above, tethered surfaces are uncrumpled and one has $L^2 \sim N$. In the case of vesicles, we expect that $\langle h^2\rangle$ is represented by the fluctuation of the mean-square radius of gyration, i.e.,

$$\langle h^2\rangle_0 \sim [\langle (\Delta R^2)^2\rangle_0]^{1/2} \equiv [\langle R^4\rangle_0 - \langle R^2\rangle_0^2]^{1/2} . \tag{10}$$

In Fig. 3, these quantities for various values of N are depicted, which exhibit $\langle (\Delta R^2)^2\rangle_0 \sim N^{1.29\pm 0.16}$. The roughness exponent is estimated to be $\zeta = 0.645\pm 0.08$ according to Eqs. (9) and (10). This result is in very good agreement with estimates from previous simulations of open polymerized membranes [12,15,16,18,20,21].

One can think of another way of estimating the roughness exponent from the fluctuation of the volume which is also given in Fig. 3 with the result $\langle (\Delta V)^2\rangle_0 \equiv \langle V^2\rangle_0 - \langle V\rangle_0^2 \sim N^{2.44\pm 0.13}$. We regard flaccid vesicles to be, on the average, a sphere of mean radius $\bar{R} \sim N^{\nu_R/2}$ and with transverse undulation h. Then one would expect

$$\langle (\Delta V)^2\rangle_0 \sim [\bar{R}^2 (\langle h^2\rangle_0)^{1/2}]^2 \sim N^{2\nu_R + \zeta} . \tag{11}$$

Putting $\nu_R = 1.0$, which yields $\zeta = 0.44\pm 0.13$, gives poor agreement with the above observation. Taking, however, the value for ν_R in Eq. (6) with its associated error, one has $\zeta = 0.54\pm 0.20$.

It has been suggested recently [22] using scaling argu-

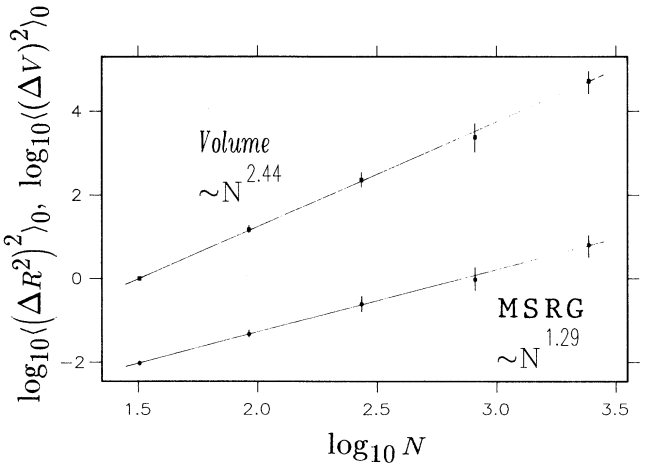

FIG. 3. Plots of the fluctuation of mean-square radius of gyration $\langle(\Delta R^2)^2\rangle_0$ and the fluctuation of volume $\langle(\Delta V)^2\rangle_0$ for the flaccid ($\Delta p=0$) polymerized vesicles as a function of number of monomers, N.

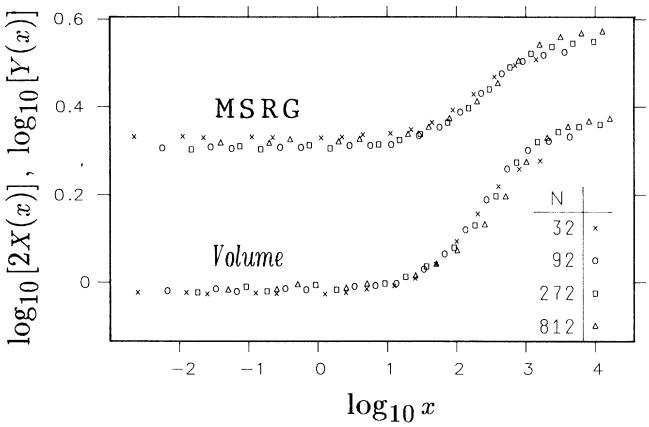

FIG. 4. Scaling plots of the mean-square radius of gyration and the volume for the inflated ($\bar{p}>0$) polymerized vesicles. Here $x=\bar{p}N^{\varphi\nu/2}$, $X=\langle R^2\rangle/A_R^2 N^{2\nu_R}$, and $Y=\langle V\rangle/A_V N^{3\nu_V/2}$ with $\varphi=1.88$, $\nu_R=0.95$ and $\nu_V=0.99$. $X(x)$ is shifted to avoid the overlap of two curves.

ments and Monte Carlo simulation that previous estimates of $\zeta=0.64$ [12,15,16,18,20,21] are probably masked by crossover effects. They observed a crossover from fluidlike behavior with $\zeta=1$ on small scales to solidlike behavior with $\zeta=\frac{1}{2}$ on large scales. $\zeta=\frac{1}{2}$ is in agreement with earlier prediction by Nelson and Peliti [23] giving finite value of the shear modulus on large scales.

Due to the large error bar in ζ estimated from the fluctuation of the volume, it is not clear whether our value could be taken as an indication for $\zeta=\frac{1}{2}$. Rather, we still think it would be more reasonable to take the former estimate $\zeta=0.645$ for our size of vesicles. This value is at least consistent with the result of field-theoretical methods, namely, the $1/d$ expansion for $(D=2)$-dimensional polymerized membranes embedded in a high d-dimensional space [25,26]. This result is $\zeta=\frac{2}{3}$ for $d=3$ and order $1/d$.

IV. INFLATED VESICLES ($\Delta p>0$)

When positive or negative constant pressure difference is applied, the shapes of vesicles deviate from flaccid configurations. The related crossover scaling forms are expected to be the analog to those for planar vesicles proposed by LSF and co-workers [6–9], i.e.,

$$\langle R^2\rangle \sim A_R^2 N^{\nu} X(x), \quad \langle V\rangle \sim A_V N^{3\nu/2} Y(x) , \tag{12}$$

where $\nu\approx 1.0$ and x is the scaled pressure variable

$$x=\bar{p}N^{\varphi\nu/2}, \quad \bar{p}\equiv\frac{\Delta p a^3}{k_B T} . \tag{13}$$

The crossover exponent φ is determined by the fluctuation of the volume at $\bar{p}=0$ [6,7] and is provided according to the linear response theorem,

$$\langle(\Delta V)^2\rangle_0 \propto \left[\frac{\partial\langle V\rangle}{\partial\bar{p}}\right]_{\bar{p}=0} \sim N^{(3+\varphi)\nu/2} . \tag{14}$$

Putting $\nu=1.0$ and using the Monte Carlo result for the fluctuation of the volume (Fig. 3) as discussed in the preceding section, one obtains $\varphi=1.88\pm0.26$. It is interesting to note that Eqs. (11) and (14) provide a relation

$$\frac{(3+\varphi)\nu}{2}=2\nu+\zeta , \tag{15}$$

and hence φ determines the crossover between the rough surface of flaccid vesicles with $\zeta\approx 0.65$ and the smooth surface of fully expanded vesicles ($\bar{p}\to\infty$) with $\zeta=0$.

For large $\bar{p}>0$, one expects that the inflated vesicle approaches its spherelike limiting shape [see Fig. 1(b)]. In Fig. 4, $X=\langle R^2\rangle/A_R^2 N^{2\nu_R}$ and $Y=\langle V\rangle/A_V N^{3\nu_V/2}$ are plotted according to the crossover scaling form Eq. (12) as a function of $x=\bar{p}N^{\varphi\nu/2}$. Using the estimated crossover exponent $\varphi=1.88$, one observes the collapsing of all the data to a single curve. This result supports the scaling forms Eq. (12).

Since $\nu\approx 1.0$ in the flaccid ($\bar{p}=0$) as well as in the inflated ($\bar{p}>0$) case, the scaling functions in Eq. (12) cannot obey a simple power law. In Fig. 4, one observes plateaus in the large x limit which arise from the finite extensibility of the tethers. We give here a rough estimate of the limiting values $X(\infty)$ and $Y(\infty)$. When vesicles are completely expanded the surface will be covered with regular triangles of length $\sqrt{2}a$. Therefore the total surface area S is approximately $S\approx\sqrt{3}Na^2$. Since the radius and the volume of a sphere are expressed in terms of surface area S as $R^2=S/4\pi$ and $V=(4\pi/3)(S/4\pi)^{3/2}$, respectively, the limiting values are given by $X(\infty)\simeq(\sqrt{3}/4\pi)/0.10=1.37$ and $Y(\infty)\simeq(1/3^{1/4}\sqrt{4\pi})/0.094=2.28$ [see Eq. (6)]. These values are in agreement with the Monte Carlo results.

It is intuitively clear that the roughness due to the fluctuations of the surface is decreased by increasing the internal pressure. In fact, according to our data $\langle(\Delta R^2)^2\rangle$ becomes independent of N with increasing $\bar{p}$.

Instead of presenting these raw data, we analyzed the fluctuation of the mean-square radius of gyration for various $\bar{p} > 0$ by the crossover scaling form

$$\langle (\Delta R^2)^2 \rangle = N^{2\zeta} f(\bar{p} N^{\phi+\zeta}) \ . \tag{16}$$

Here $f(y)$ is a scaling function with $f(y)=$const for $y \ll 1$. In this limit $\langle (\Delta R^2)^2 \rangle$ reduces to Eq. (9) for flaccid vesicles. Fixing $\zeta=0.645$, we obtained the best overlap of data if $\phi=0.05\pm0.03$. This is presented in Fig. 5, where $f=\langle (\Delta R^2)^2 \rangle / N^{2\zeta}$ is shown as a function of $y=\bar{p} N^{\phi+\zeta}$. Our results yield a power-law behavior of the scaling function according to $f(y) \sim 1/y^2$ for $y \gg 1$.

This power law can be understood by the following argument. The configuration of a nearly flat polymerized membrane with surface tension $\sigma \sim \bar{p} N^{\phi}$ is described by two in-plane phonon-displacement fields, $\mathbf{u}(x_1,x_2)$, and an out-of-plane displacement field, $h(x_1,x_2)$. The strain tensor u_{ij} has the form [24]

$$u_{ij} = \tfrac{1}{2}[\partial_i u_j + \partial_j u_i + (\partial_i h)(\partial_j h)] \ , \tag{17}$$

with $\partial_i \equiv \partial x_i$ and $i,j=1,2$, and the elastic energy is given by [23]

$$H(\mathbf{u},h) = \tfrac{1}{2}\int d^2x [\sigma(\nabla h)^2 + \kappa_0 (\nabla^2 h)^2] + \tfrac{1}{2}\int d^2x (2\mu u_{ij}^2 + \lambda u_{kk}^2) \ , \tag{18}$$

where μ,λ are Lamé coefficients. Because of the nonlinear coupling between $\mathbf{u}$ and h, the effective long-wavelength bending rigidity differs from their microscopic value; effective bending rigidity is scale dependent [19,21,23,25,26],

$$\kappa_{\rm eff}(q) \sim \frac{\kappa_0}{q^{\eta}}, \quad 0 \le \eta < 2 \tag{19}$$

for small q. Assuming that σ is not renormalized by this nonlinear coupling, we obtain the out-of-plane fluctuation from the equipartition theorem

$$\langle h^2 \rangle \approx \frac{k_B T}{2\pi} \int_{q_{\rm min}}^{q_{\rm max}} \frac{1}{\sigma q^2 + \kappa_{\rm eff} q^4} dq \approx \frac{k_B T}{2(2-\eta)\pi\sigma} \ln\left[1 + \frac{\sigma}{\kappa_0 q_{\rm min}^{2\zeta}}\right], \quad \zeta = \frac{2-\eta}{2} \ . \tag{20}$$

This integral diverges at its lower limit $q_{\rm min} \sim N^{-1/2}$. Equation (20) implies that the quantity $\langle h^2 \rangle / N^{\zeta}$ depends only on the variable σN^{ζ}. The case of fluid membranes [27,28] with surface tension [29] can be easily recovered by putting $\eta=0$. The two limiting cases for $\sigma \to 0$ [19] and $\sigma \to \infty$ are

$$\langle h^2 \rangle \sim \frac{k_B T}{\kappa_0} N^{\zeta} \tag{21}$$

and

$$\langle h^2 \rangle \sim \frac{k_B T}{\kappa_0} \ln \frac{\sigma N^{\zeta}}{\kappa_0} \ , \tag{22}$$

respectively. Equation (22) shows the power-law dependence of the quantity $\langle h^2 \rangle / N^{\zeta}$ on σN^{η}.

In the case of closed membranes (vesicles), the surface tension depends on the vesicle size according to [8,9]

$$\sigma = \tfrac{1}{2} \Delta p \bar{R} \sim \Delta p N^{1/2} \ , \tag{23}$$

i.e., $\phi=0.5$, which is not consistent with our result. This discrepancy probably indicates a local dependency of the surface tension which is not included in the present argument.

V. DEFLATED VESICLES ($\Delta p < 0$)

Monte Carlo results for deflated vesicles with $\bar{p} < 0$ are analyzed by the same crossover scaling forms as given in Eq. (12). However, it was necessary to employ a different crossover exponent $\varphi' = 4.40 \pm 0.20$ in order to obtain a collapse of all the data on a single curve. We estimated this value from several attempts to obtain optimal overlap of the curves for all values of N. Scaling plots with $\varphi' = 4.40$ are depicted in Fig. 6. One observes power laws for $|x| > 10^4$:

$$X(x) \approx \frac{X_-}{|x|^{\rho}}, \quad Y(x) \approx \frac{Y_-}{|x|^{\tau}} \ , \tag{24}$$

with $\rho = 0.140 \pm 0.007$ and $\tau = 0.185 \pm 0.008$. These results imply that $\langle R^2 \rangle \sim N^{\nu_R^-}$ and $\langle V \rangle \sim N^{3\nu_V^-/2}$ with $\nu_R^- = \nu_R(1 - \varphi'\rho/2) = 0.66 \pm 0.08$ and $3\nu_V^-/2 = (3\nu_V/2)(1 - \varphi'\tau/3) = 1.08 \pm 0.08$.

Our result for ν_R^- is very close to the lower limiting value for the correlation length exponent ν, corresponding to the "fully collapsed" configuration. The exponent ν for a self-avoiding D-dimensional surface in d-dimensional space should generally satisfy

$$\frac{D}{d} \le \nu \le 1 \ , \tag{25}$$

which is in our case $\frac{2}{3} \le \nu \le 1$. This compact structure is also observed by the exponent for the volume, $3\nu_V^-/2$, since $\langle V \rangle \sim N a^3$ is expected for this configuration. In

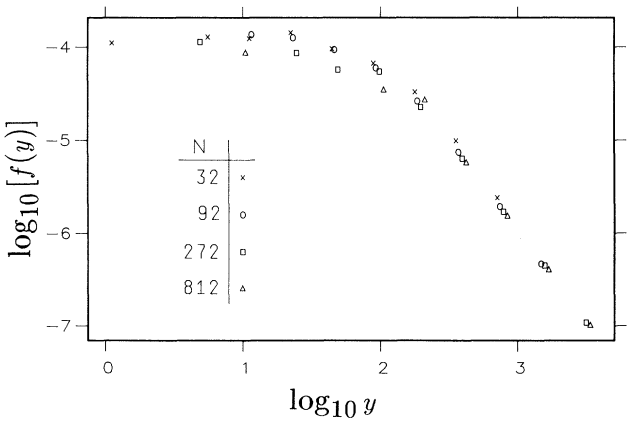

FIG. 5. Scaling plot of the fluctuation of mean-square radius of gyration for the inflated ($\bar{p} > 0$) polymerized vesicles. Here $y = \bar{p} N^{\phi+\zeta}$ and $f = \langle (\Delta R^2)^2 \rangle / N^{2\zeta}$ with $\phi = 0.05$ and $\zeta = 0.645$.

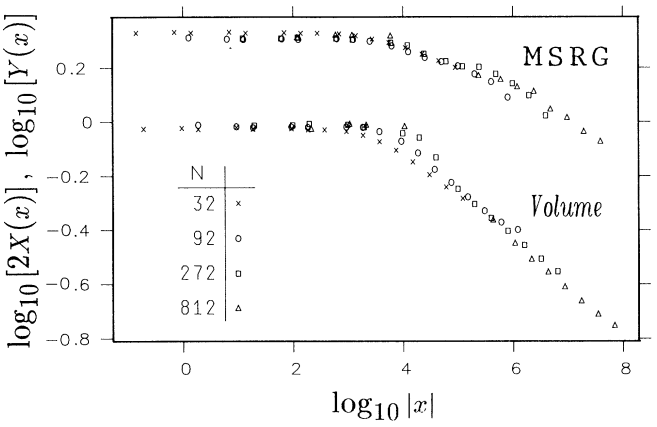

FIG. 6. Scaling plots of the mean-square radius of gyration and the volume for the deflated ($\bar{p}<0$) polymerized vesicles. Here $|x|=|\bar{p}N^{\varphi'\nu/2}|$, $X=\langle R^2\rangle A_R^2 N^{\nu_R}$ and $Y=\langle V\rangle/A_V N^{3\nu_V/2}$ with $\varphi'=4.40$, $\nu_R=0.95$, and $\nu_V=0.99$. $X(x)$ is shifted to avoid the overlap of two curves.

other words, our results show that the fractal dimension of deflated vesicles is $d_f=3$, which is related to ν by $d_f=D/\nu$.

This is in contrast to planar deflated ($D=1$)-dimensional vesicles [6,7], which exhibit conformations matching the structure of branched polymers with $\nu\approx 0.62$. Since the corresponding exponent for branched polymers in ($d=3$)-dimensional space is $\nu=1.0$ [30–32] (note that the definition of ν in the case of membranes is twice that for polymers), our result $\nu_R^- \approx 0.66$ for deflated ($D=2$)-dimensional vesicles indicates that the related conformations must resemble more closed-packed structures rather than ramified arrangements. This is also supported by a typical snapshot of a deflated vesicle presented in Fig. 1(c).

Abraham and Nelson investigated self-avoiding tethered surfaces by molecular-dynamics simulation also, in the presence of Lennard-Jones-type attractive interaction between monomers [18]. Their scaling analysis of the structure function gives the correlation exponent $\nu=\frac{2}{3}$ characteristic of a collapsed object. This value has been indeed observed for deflated vesicles in our simulation. As they point out in their paper, it is remarkable that we can obtain a compact phase for self-avoiding finite thickness membranes by a simulation in spite of the previous difficulties [3,33].

It should be noted that the difference between $\varphi'\approx 4.4$ and $\varphi\approx 1.88$ [Eq. (15)] determining crossovers in the deflated and inflated regimes, respectively, is due to the difference in the crossover phenomena concerned; while φ' is related to the change of $\nu=1.0$ to $\nu^-\approx 0.66$, the exponent φ is related to the change of $\zeta\approx 0.65$ to 0.

VI. DYNAMICS

In the following section we discuss some dynamical properties of polymerized vesicles at constant pressure. We restrict our attention to the time-dependent correlation function of the mean-square radius of gyration

$$\Phi(t)=\frac{\langle R^2(0)R^2(t)\rangle-\langle R^2\rangle^2}{\langle R^4\rangle-\langle R^2\rangle^2}\ .$$

This is depicted in Figs. 7, 8, and 9 for $p=0$, 4, and -4, respectively. In order to estimate typical relaxation times $\tau\sim N^w$ for the various cases, and assuming for the slowest mode $\Phi(t/\tau)$ to be approximately independent of N, we have fitted an *effective* exponent w by attempting to find the best overlaps of $\Phi(t)$ versus t/τ for each of the three cases of p.

In the case where no pressure is applied ($\bar{p}=0$), one would expect to observe a Rouse-type behavior, $\tau\sim N^{1+\nu}$, which has been explained in detail for open polymerized membranes by Kantor, Kardar, and Nelson [3]. However, according to our data for $\Phi(t)$ versus t/N^2 (since $\nu\approx 1$) as depicted in Fig. 7a, this Rouse-type behavior is not observed, but rather a relaxation with $\tau\sim N$ is detected for $t/N<10$, which is presented in Fig. 7(b). A possible explanation for this finding must be related to the fact that the vesicle at $\bar{p}=0$ is not flaccid, in which case we would expect a Rouse-type relaxation, but only rough, which requires separate considerations of in-plane and

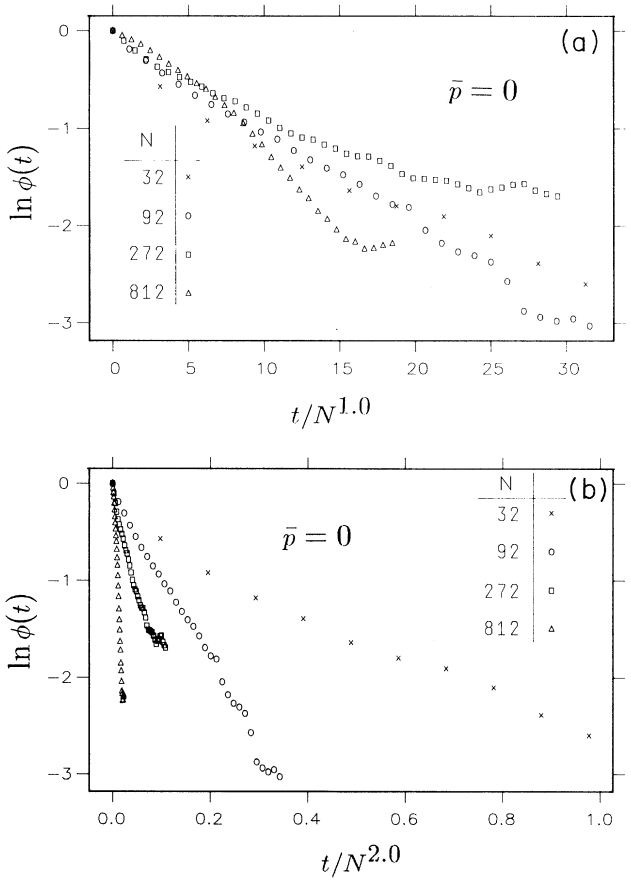

FIG. 7. (a) Time correlation function $\Phi(t)$ of the mean-square radius of gyration vs scaled time t/N^2 for the rough ($\bar{p}=0$) polymerized vesicles. (b) Time correlation function $\Phi(t)$ vs scaled time t/N for the rough ($\bar{p}=0$) polymerized vesicles.

out-of-plane time correlation functions. For in-plane longitudinal relaxation we expect $\tau_u \sim N$, similar to the case of permanent cross-linked networks [34], whereas for out-of-plane relaxation $\tau_h \sim N^{1+\zeta}$. Assuming that $\Phi(t)$ can be reasonably represented by the sum of two exponentials

$$\Phi(t) \sim A_u \exp(-t/\tau_u) + A_h \exp(-t/\tau_h) ,$$

our data in Fig. 7(b) might be interpreted to indicate $A_u/A_h \gg 1$, which would explain the dominance of in-plane relaxation, at least for small N. Of course, according to this argument, for very large N, we must expect the out-of-plane fluctuations to become the more important relaxation mechanism for rough vesicles. Estimates of τ_u and τ_h separately can be obtained by simulations of open polymerized membranes.

The scaled relaxation function for *inflated* vesicles is presented in Fig. 8. For simplicity we have restricted our attention to $\bar{p}=4.0$, where the vesicles have almost assumed their fully expanded shape [compare Fig. 1(b)]. The effective exponent is approximately $w \approx 0.4$. An almost exponential decay is observed over three time intervals of the order of $40N^{0.4}$, which can be considered to be sufficient for obtaining equilibrated data of various static quantities. We have not undertaken to develop a theoretical explanation for the effective exponent $w=0.4$. In order to characterize in general the relaxation of inflated vesicles, one would have to consider the crossover behavior between the rough and the inflated (flat) case, in the same way as has been demonstrated above for static quantities [see, e.g., Eqs. (12) and (13)]. This is not within the scope of the present paper and is left to subsequent work.

In Fig. 9, the scaled relaxation functions for *deflated* vesicles at $\bar{p}=-4$ are presented. Assuming Rouse-type relaxation [3] with $\tau \sim N^{1+\nu}$, we have scaled the time according to $t/N^{5/3}$, corresponding to $\nu \approx \frac{2}{3}$ for deflated vesicles. The relaxation is, as expected, very slow as compared to the relaxation of rough or inflated vesicles. For small vesicles ($N=32,92$), the decay of the correlation functions according to Fig. 9 seems to give support for

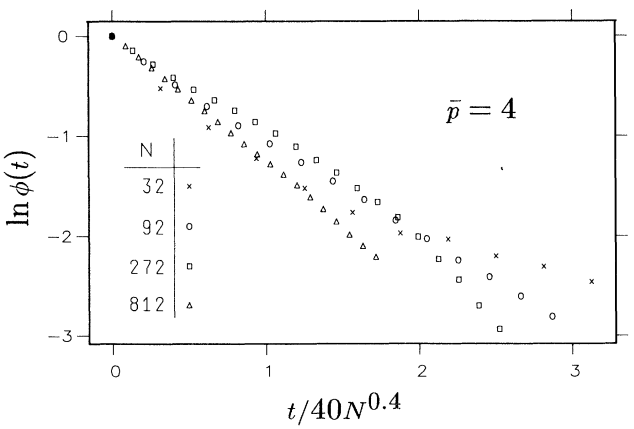

FIG. 8. Time correlation function $\Phi(t)$ vs scaled time t/τ for inflated ($\bar{p}=4$) polymerized vesicles of various sizes N.

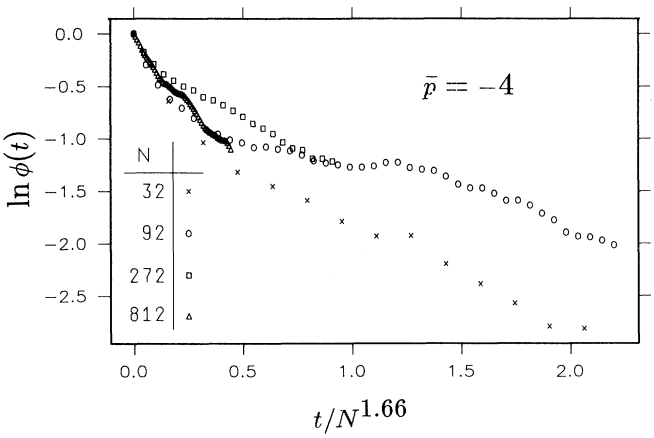

FIG. 9. Time correlation function $\Phi(t)$ vs scaled time t/τ for deflated ($\bar{p}=-4$) polymerized vesicles of various sizes N.

well-equilibrated static quantities, whereas for larger vesicles the data of static quantities, as discussed in Sec. V, might be taken with some reservations with respect to represent uncorrelated ensembles. Crossover scaling analysis for $\Phi(t)$ must therefore fail. Separate Monte Carlo investigations to the dynamics of deflated polymerized vesicles are required.

VII. SUMMARY AND CONCLUSION

This work can be summarized as follows.

We have performed Monte Carlo simulations for polymerized vesicles at various constant pressure differences Δp. Flaccid vesicles ($\Delta p=0$) exhibit uncrumpled configurations with a mean-square radius of gyration $\langle R^2 \rangle_0 \sim N^{\nu}$ and the volume $\langle V \rangle_0 \sim N^{3\nu/2}$, where $\nu \approx 1.0$. Here N is the number of monomers and is proportional to the surface area. The surface of flaccid vesicles is rough and the related roughness exponent $\zeta=0.645\pm0.08$, estimated from the fluctuation of the mean-square radius of gyration, is in good agreement with other simulation results.

We presented a crossover scaling analysis for the mean-square radius of gyration and the mean volume for inflated ($\Delta p>0$) and deflated ($\Delta p<0$) vesicles. The crossover to inflated vesicles ($\nu=1.0$) is governed by the successive reduction of the corrugation due to the pressure, i.e., from $\zeta=0.65$ to 0 in the asymptotic limit. This crossover is characterized by an exponent $\varphi=1.88$. Inflated vesicles become expanded spheres.

On the other hand, the crossover to deflated vesicles, characterized by the exponent $\varphi'=4.4$, is ruled by the change of their sizes. The correlation length exponent changes from $\nu=1.0$ to 0.66 with which deflated vesicles exhibit fully collapsed configuration.

ACKNOWLEDGMENTS

One of us (S.K.) is very grateful for the hospitality of IFF at Forschungszentrum Jülich. We would like to express our appreciation to Professor R. Lipowsky and Dr. Y. Taguchi for their interest and useful comments. This work was done on a Cray X-MP/416.

*Present address: Institute of Physics, College of Arts and Sciences, University of Tokyo, Meguro-ku, Tokyo 153, Japan.

[1] See, for instance, *Statistical Mechanics of Membranes and Surfaces,* Proceedings of the Fifth Jerusalem Winter School, edited by D. R. Nelson, T. Piran, and S. Weinberg (World Scientific, Singapore, 1989).
[2] K. Berndl, J. Käs, R. Lipowsky, E. Sackmann, and U. Seifert, Europhys. Lett. **13**, 659 (1990).
[3] Y. Kantor, M. Kardar, and D. R. Nelson, Phys. Rev. Lett. **57**, 791 (1986); Phys. Rev. A **35**, 3056 (1987).
[4] Y. Kantor and D. R. Nelson, Phys. Rev. Lett. **58**, 2774 (1987); Phys. Rev. A **36**, 4020 (1987).
[5] A. Baumgärtner and J.-S. Ho, Phys. Rev. A **41**, 5747 (1990).
[6] S. Leibler, R. R. P. Singh, and M. E. Fisher, Phys. Rev. Lett. **59**, 1989 (1987).
[7] M. E. Fisher, Physica (The Hague) D **38**, 112 (1989).
[8] C. J. Camacho and M. E. Fisher, Phys. Rev. Lett. **65**, 9 (1990).
[9] A. C. Maggs, S. Leibler, M. E. Fisher, and C. J. Camacho, Phys. Rev. A **42**, 691 (1990).
[10] S. Komura and A. Baumgärtner, J. Phys. (Paris) **51**, 2395 (1990).
[11] R. M. Neumann, Phys. Rev. A **31**, 3516 (1985).
[12] M. Plischke and D. Boal, Phys. Rev. A **38**, 4943 (1988).
[13] F. F. Abraham, W. E. Rudge, and M. Plischke, Phys. Rev. Lett. **62**, 1757 (1989).
[14] J.-S. Ho and A. Baumgärtner, Phys. Rev. Lett. **63**, 1324 (1989).
[15] D. Boal, E. Levinson, D. Liu, and M. Plischke, Phys. Rev. A **40**, 3292 (1989).
[16] J.-S. Ho and A. Baumgärtner, Europhys. Lett. **12**, 295 (1990).
[17] B. Duplantier, Phys. Rev. Lett. **64**, 493 (1990).
[18] F. F. Abraham and D. R. Nelson, J. Phys. (Paris) **51**, 2653 (1990).
[19] R. Lipowsky, Europhys. Lett. **7**, 255 (1988).
[20] S. Leibler and A. C. Maggs, Phys. Rev. Lett. **63**, 406 (1989).
[21] E. Guitter, S. Leibler, A. C. Maggs, and F. David, J. Phys. (Paris) **51**, 1055 (1990).
[22] R. Lipowsky and M. Girardet, Phys. Rev. Lett. **65**, 2893 (1990).
[23] D. R. Nelson and L. Peliti, J. Phys. (Paris) **48**, 1085 (1987).
[24] L. D. Landau and E. M. Lifshitz, *Theory of Elasticity* (Wiley, New York, 1970).
[25] J. A. Aronovitz and T. C. Lubensky, Phys. Rev. Lett. **60**, 2634 (1988).
[26] E. Guitter, F. David, S. Leibler, and L. Peliti, J. Phys. (Paris) **50**, 1787 (1989).
[27] W. Helfrich, J. Phys. (Paris) **46**, 1263 (1985).
[28] L. Peliti and S. Leibler, Phys. Rev. Lett. **54**, 1690 (1985).
[29] W. Helfrich and R. Servuss, Nuovo Cimento D **3**, 137 (1984).
[30] J. Isaacson and T. C. Lubensky, J. Phys. (Paris) Lett. **41**, L469 (1980).
[31] M. Daoud and J. F. Joanny, J. Phys. (Paris) **42**, 1359 (1981).
[32] G. Parisi and N. Sourlas, Phys. Rev. Lett. **46**, 871 (1981).
[33] M. A. F. Gomes and G. L. Vasconcelos, Phys. Rev. Lett. **60**, 238 (1988); Y. Kantor, M. Kardar, and D. R. Nelson, *ibid.* **60**, 239 (1988).
[34] P. G. de Gennes, Macromolecules **9**, 587 (1976).